

Nonohmicity and energy relaxation in diffusive two-dimensional metals

Roy Ceder, Oded Agam, and Zvi Ovadyahu

Racah Institute of Physics, The Hebrew University, Jerusalem 91904, Israel

(Received 24 May 2005; revised manuscript received 27 September 2005; published 7 December 2005)

We analyze current-voltage characteristics taken on Au-doped indium-oxide films. By fitting a scaling function to the data, we extract the electron-phonon scattering rate as function of temperature. Consistently good fits are obtained for both short-sample and long-sample limits using data of the same material. The fitting implies a quadratic dependence of the electron-phonon scattering rate on temperature from 1 down to 0.28 K. The origin of this enhanced electron-phonon scattering rate is ascribed to the mechanism proposed by Sergeev and Mitin.

DOI: [10.1103/PhysRevB.72.245104](https://doi.org/10.1103/PhysRevB.72.245104)

PACS number(s): 72.15.Lh, 72.10.-d, 73.61.-r, 63.20.Kr

I. INTRODUCTION

Energy relaxation processes play an important role in the low-temperature transport properties of diffusive metals, alloys and semiconductors. In particular, they determine the maximum electric field F allowed if the system is to be measured under near-equilibrium conditions at a given temperature. The condition for that may be expressed as $eFL_\epsilon \ll k_B T$ where the energy relaxation length L_ϵ is the length over which the electron diffuses under F before the energy gained from it is dissipated into the thermal bath. In particular, this issue is relevant for all aspects of quantum transport such as corrections to the conductivity due to interference and electron-electron interactions. For a system of size $L \gg L_\epsilon$, energy relaxation processes are usually controlled by electron-phonon inelastic scattering, and in the following we shall assume that L_ϵ is dominated by the electron-phonon diffusion length L_{ep} . Note that other forms of inelastic scattering, such as electron-electron and electron-two-level systems, while acting as sources of dephasing (actually, they are usually the dominant source of dephasing at low temperatures), are ineffective as energy relaxation agents in the context used here. We shall further comment on this issue in the discussion section.

In clean samples the electron-phonon scattering mechanism is well understood and the scattering rate τ_{ep}^{-1} , is known to be proportional to T^3 (where T denotes the temperature). In dirty systems, however, where the elastic mean free path of the electron is smaller than the phonon thermal length, the situation is more complicated. Schmid¹ showed that in this case τ_{ep}^{-1} is suppressed and becomes proportional to T^4 , in accordance with Pipard's ineffectiveness condition.² His model assumed that the impurities are anchored to the lattice, and the scattering rate was calculated by moving into a reference frame which follows the lattice vibrations. Riezer and Sergeev obtained the same result using the laboratory reference frame.³ A scattering rate proportional to T^4 has indeed been observed in a number of experiments.⁴⁻⁶ However, a T^3 law was frequently observed even in systems that were presumably well into the dirty limit regime.⁷⁻¹⁰ Moreover, quite a few observations of a T^2 scattering law were reported in other experiments.¹¹⁻¹⁴ The latter experimental results triggered further studies with the aim of understanding better the

electron-phonon scattering mechanism in disordered metals. In particular, to obtain an electron-phonon scattering rate proportional to T^2 (rather than the "ineffective" T^4 law), Belitz and Wybourne¹⁵ assumed a strong phonon damping, while Jan Wu and Wei¹⁶ included effects associated with the discrete lattice structure. Sergeev and Mitin¹⁷ obtained the T^2 behavior from a model where impurities are assumed to be fixed, namely, impurities which do not follow the lattice vibrations. They argued that heavy impurities or boundaries which move differently from the host lattice produce the same effect.

In this paper we analyze the non-ohmic characteristic of thin films of $\text{In}_2\text{O}_{3-x}:\text{Au}$ (crystalline indium-oxide doped with 2% gold), that were characterized and measured as described elsewhere.¹⁸ We show that in this system $\tau_{ep}^{-1} \propto T^2$, and interpret this behavior as a manifestation of the Sergeev Mitin mechanism where the Au atoms play the role of the "immobile impurities." The sample resistance is used as a thermometer of the electron temperature (see Ref. 18 for limitations of this assumption). The latter is determined by the energy balance between the Joule heating, due to the presence of electric field, and the heat transfer to the lattice phonons governed by τ_{ep}^{-1} .

The data we shall analyze are traces of the differential-resistance R versus voltage for a typical film at $T \leq 1$ K shown in Fig. 1 (top panel). As expected, the deviations from Ohm's law become more pronounced as T decreases. In the bottom panel of Fig. 1 it is shown that these curves taken at different temperatures can be collapsed into a common function

$$\frac{\Delta R}{R} \equiv \frac{R(F, T) - R(0, T)}{R(0, T)} = \Delta \mathcal{R}_p \left(\frac{F}{T^{p/2+1}} \right) \quad (1)$$

with $p=2$. The scaling of the electric field as a power of the temperature $F \sim T^{p/2+1}$ and its relation to the electron-phonon time $\tau_{ep}^{-1}(T) \propto T^p$, has been already recognized by Anderson, Abrahams, and Ramakrishnan,¹⁹ and later by Arai.²⁰ In the next section we shall calculate the function $\Delta \mathcal{R}_p$, and clarify its relation to the electron-phonon relaxation time. We shall consider the dependence on the sample length and compare with further experimental results in Sec. III.

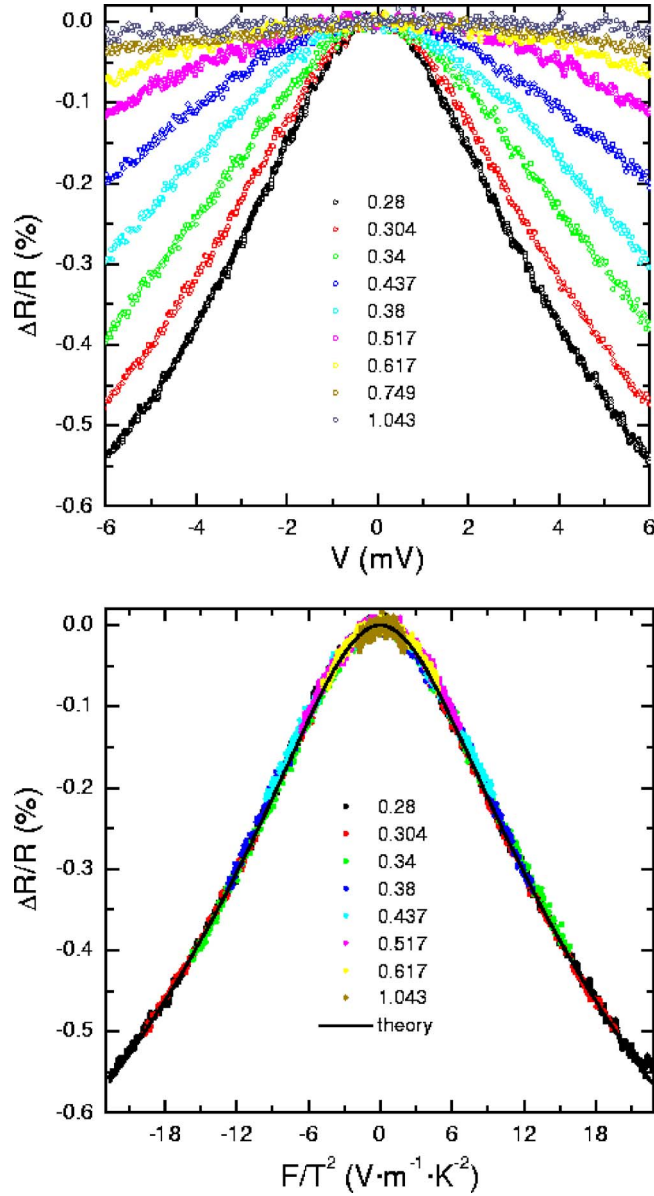


FIG. 1. (Color online) The fractional change in the nonohmic characteristic of 200-Å-thick $\text{In}_2\text{O}_{3-x}:\text{Au}$ sample measured at different temperatures (marked on each curve). Sample length is $L = 3500 \mu\text{m}$ and width $W = 1 \text{ mm}$. Top panel: The differential resistance [defined in Eq. (1) as a function of the voltage]. Bottom panel: The same data plotted as function of $F(=V/L)$ normalized by T^2 . Note the near perfect data collapse as well as the fit to formula (20) represented by the continuous line.

II. THEORY

The essence of the picture developed below is the assignment of an effective temperature for a given field and bath-temperature. The electrons are accelerated by the electric field, and the collisions with other electrons and phonons result in a local equilibrium distribution characterized by an effective temperature T_{eff} . The latter differs from the bath temperature T , and depends on the electric field. We shall make the association $R(F, T) \approx R(0, T_{\text{eff}})$. Hence knowing $T_{\text{eff}}(F, T)$ and the form of the near-equilibrium $R(0, T)$ yields

the desired $R(F, T)$ from which we deduce the scaling function (1).

We begin by considering the Boltzmann equation for the electron distribution function f :

$$\frac{\partial f}{\partial t} + \vec{v} \cdot \frac{\partial f}{\partial \vec{r}} + e\vec{F} \cdot \frac{\partial f}{\partial \vec{p}} = I[f]. \quad (2)$$

Here \vec{r} is the position, \vec{v} is the velocity, \vec{p} denotes the momentum, \vec{F} the electric field, and $I[f] = I_{\text{im}}[f] + I_{\text{ee}}[f] + I_{\text{ep}}[f, N]$ represents the collision integrals due to impurity scattering, electron-electron, and electron-phonon interactions. The latter depends also on the phonon distribution function, assumed to be the equilibrium distribution function denoted by N .

Following Nagaev²¹ and Kozub and Rudin,²² we look for a steady state solution of the form

$$f = f(\vec{r}, \hat{n}, \epsilon - e\vec{F} \cdot \vec{r}), \quad (3)$$

where \hat{n} denotes a unit vector in the direction of the momentum, and $\epsilon = \epsilon(p)$ is the energy assumed to depend on the absolute value of the momentum $p = |\vec{p}|$. Substituting Eq. (3) into Eq. (2) leads to

$$\vec{v} \cdot \frac{\partial f}{\partial \vec{r}} + \sum_{ij} \frac{eF_i}{p} (\delta_{ij} - n_i n_j) \frac{\partial f}{\partial n_j} = I[f]. \quad (4)$$

Next, we define the symmetric and anti-symmetric parts of the distribution function with respect to the momentum direction $f^\pm = [f(\hat{n}) \pm f(-\hat{n})]/2$, and construct two new equations from Eq. (4) associated with the addition and subtraction of Boltzmann equations for $f(\hat{n})$ and $f(-\hat{n})$. Then assuming that momentum relaxation is dominated by scattering from impurities, and that electron-electron and electron-phonon interactions are essentially independent of the momentum direction (i.e., $I_{\text{ee}}[f] \approx I_{\text{ee}}[f^+]$, and $I_{\text{ep}}[f, N] \approx I_{\text{ep}}[f^+, N]$), we obtain

$$\vec{v} \cdot \frac{\partial f^\pm}{\partial \vec{r}} + \sum_{ij} \frac{eF_i}{p} (\delta_{ij} - n_i n_j) \frac{\partial f^\pm}{\partial n_j} = \bar{I}[f^\pm], \quad (5)$$

where $\bar{I}[f^\pm] \approx I_{\text{ee}}[f^\pm] + I_{\text{ep}}[f^\pm, N]$, and

$$\vec{v} \cdot \frac{\partial f^\pm}{\partial \vec{r}} = I_{\text{im}}[f^\pm]. \quad (6)$$

In the simplest approximation, the impurity collision term takes the form $I_{\text{im}}[f^\pm] = -f^\pm/\tau$, where τ is the elastic mean free time. Thus using Eq. (6), the antisymmetric part of the distribution function can be expressed in terms of the symmetric part and substituted into Eq. (5). The resulting equation is now averaged over the momentum directions to give

$$-D\nabla^2 f^+ = I_{\text{ee}}[f^+] + I_{\text{ep}}[f^+, N], \quad (7)$$

where $D = \tau v_F^2/3$ is the diffusion constant (v_F is the Fermi velocity). Here and henceforth we neglect the energy dependence of the diffusion constant.

We wish to solve Eq. (7) for homogeneous samples with voltage contacts located at $x = \pm L/2$. Thus f^+ is independent of the transverse coordinates, and the boundary conditions assuming ideal contacts are

$$f^+|_{x=\pm L/2} = n_F \left(\frac{\epsilon - \epsilon_F \mp \frac{eV}{2}}{k_B T} \right), \quad (8)$$

where $n_F(\epsilon) = [1 + \exp(\epsilon)]^{-1}$ is the Fermi distribution function, ϵ is the electron energy, ϵ_F is the Fermi energy, $V = FL$ is the voltage drop across the sample, k_B is Boltzmann constant, and T is the bath temperature.

Equation (7) is a nonlinear equation for the electron distribution function. To make progress, we shall assume that the electron-electron diffusion length L_{ee} is much smaller than the system size L and the energy relaxation length L_{ep} . This should secure an effective local thermalization due to the large number of collisions an electron experiences. We looking then for a solution which describes local equilibrium of the electrons

$$f^+ = n_F \left(\frac{\epsilon - \epsilon_F - eFx}{k_B T_{\text{loc}}(x)} \right), \quad (9)$$

where $T_{\text{loc}}(x)$ is a local temperature of the electrons. At the contacts the local temperature by assumption coincides with the bath temperature

$$T_{\text{loc}} \left(\pm \frac{L}{2} \right) = T, \quad (10)$$

so that the solution (9) with the boundary conditions (10) satisfies the requirement (8). Under the assumption of local equilibrium the electron-electron collision term vanishes and Eq. (7) reduces to

$$-D \frac{\partial^2 f^+}{\partial x^2} = I_{ep}[f^+, N]. \quad (11)$$

Finally, to extract the local temperature behavior we multiply this equation by ϵ and integrate over the energy. The resulting equation is

$$D \left[\frac{\pi^2 k_B^2}{6} \frac{\partial T_{\text{loc}}^2(x)}{\partial x^2} + (eF)^2 \right] = - \int d\epsilon \epsilon I_{ep}[f^+, N]. \quad (12)$$

To further simplify Eq. (12), we take the electron-phonon collision integral to have the form

$$I_{ep} = \int d\omega K(\omega) \left\{ - (1 - f^+(\epsilon + \omega)) f^+(\epsilon) N \left(\frac{\omega}{k_B T} \right) + [1 - f^+(\epsilon)] \right. \\ \times f^+(\epsilon + \omega) \left[N \left(\frac{\omega}{k_B T} \right) + 1 \right] - [1 - f^+(\epsilon - \omega)] f^+(\epsilon) \\ \left. \times \left[N \left(\frac{\omega}{k_B T} \right) + 1 \right] + [1 - f^+(\epsilon)] f^+(\epsilon - \omega) N \left(\frac{\omega}{k_B T} \right) \right\}, \quad (13)$$

where $K(\omega) = \alpha \omega^{p-1}$, is a kernel depending on the nature of the collision between the electrons and phonons, while $N(\omega/k_B T) = [\exp(\omega/k_B T) - 1]^{-1}$ is the equilibrium phonon distribution function. We substitute this expression into Eq. (12) with the approximate local equilibrium form of the electron distribution function (9), and integrate over ϵ and ω . The resulting equation is an equation for the local temperature

$$\frac{\pi^2 k_B^2}{6} \frac{\partial T_{\text{loc}}^2(x)}{\partial x^2} + (eF)^2 = \eta k_B^{p+2} [T_{\text{loc}}^{p+2}(x) - T^{p+2}], \quad (14)$$

where

$$\eta = (1 - 2^{-(p+1)})(p+1)! \zeta(p+2) \frac{\alpha}{D}. \quad (15)$$

In understanding the form of the solution of Eq. (14), it is instructive to identify first the relevant length scale for this equation. To this end one may linearize the equation by substituting $T_{\text{loc}}^2(x) = T^2 + \delta T^2(x)$ and expanding to linear order in $\delta T^2(x)$. The solution of the resulting equation with the boundary conditions (10) is

$$T_{\text{loc}}^2(x) = T^2 + \frac{6(eFL_{ep})^2}{k_B^2 \pi^2} \left(1 - \frac{\cosh\left(\frac{x}{L_{ep}}\right)}{\cosh\left(\frac{L}{2L_{ep}}\right)} \right), \quad (16)$$

where

$$L_{ep} = \frac{\pi(k_B T)^{-p/2}}{\sqrt{3(p+2)\eta}} \quad (17)$$

is essentially the electron-phonon length at equilibrium. From Eq. (16) one can see that L_{ep} sets the distance from the contacts over which the temperature profile reaches a saturated value. Thus long sample satisfies $L \gg L_{ep}$, and these may be considered to have an essentially space independent local temperature which we shall refer to as the effective temperature.

The linearized solution for long samples (16) is strictly justified when the electric field is weak, i.e., $eFL_{ep} < k_B T$. We shall be interested in the limit of strong fields where L_{ep} will presumably be smaller than its equilibrium value, the right-hand side (RHS) of (17). Provided $L \gg L_{ep}(T, F)$ it makes sense to assume an electron temperature which is essentially constant throughout the sample. We then neglect the space dependent term in Eq. (14), and the effective temperature of the electrons, at any field strength, is readily deduced to be

$$T_{\text{eff}} \simeq \left[T^{p+2} + \frac{(eF)^2}{\eta k_B^{p+2}} \right]^{1/(p+2)}. \quad (18)$$

As mentioned earlier, once T_{eff} is known, to find the scaling function $\Delta \mathcal{R}_p$ requires only the temperature dependence of the resistance $R(T)$ since $R(F, T) \simeq R(0, T_{\text{eff}})$. At low temperatures, the temperature dependent terms of the resistance are the weak localization²³ and the Altshuler-Aronov corrections.²⁴ For thin films, both of these have a logarithmic behavior, thus

$$R(0, T) \simeq R_D [1 - \gamma \ln(T)], \quad (19)$$

where γ is a small dimensionless constant, depending on the nature of the electron-electron interactions, the spin-orbit coupling, and the ratio of the quantum unit resistance to the Drude resistance of the sample R_D . Substituting $R(F, T) \simeq R(0, T_{\text{eff}})$ and Eq. (19) in the definition of the scaling function (1), and expanding to the leading order in γ we obtain

$$\Delta\mathcal{R}_p\left(\frac{F}{T^{p/2+1}}\right) \approx -\frac{\gamma}{p+2} \ln\left[1 + \frac{(eF)^2}{\eta(k_B T)^{p+2}}\right]. \quad (20)$$

Note that this has the scaling form as in Eq. (1) above.

To anticipate the discussion in the next section, it is instructive to consider the case of short samples $L_{ep} \gg L$. Here one may neglect the contribution of the electron-phonon collision term in Eq. (12) and readily obtain the solution for $T_{loc}(x)$, whose space dependence, in general, cannot be ignored:

$$T_{loc}^2(x) = T^2 + \frac{3(eF)^2}{k_B^2 \pi^2} \left(\frac{L^2}{4} - x^2\right). \quad (21)$$

At the temperature range where the dephasing length is much smaller than the system size one may view the sample as a set of classical resistors connected in series. Therefore the total resistance can be approximated by the sum $R(F, T) \approx \sum_j R_j$, where $R_j = R[T_{loc}(x_j)]$ is the resistance of the j th segment (of size of the dephasing length), centered at the point x_j . Thus, assuming homogeneous sample, the experimentally measured resistivity is essentially an average over the position. From this average one immediately obtains the scaling function of short samples

$$\Delta\mathcal{R}_0\left(\frac{V}{T}\right) \approx -\gamma \left[\chi \tanh^{-1}\left(\frac{1}{\chi}\right) - 1 \right], \quad (22)$$

where

$$\chi = \sqrt{1 + \frac{4\pi^2}{3} \left(\frac{k_B T}{eV}\right)^2} \quad (23)$$

and $V = FL$ is the voltage drop along the sample.

III. DATA ANALYSIS AND DISCUSSION

Comparing the resistance curves shown in Fig. 1 with Eq. (20), one notes that a scaling form that leads to the data collapse occurs for $p=2$. This means that the energy relaxation time is quadratic with temperature: $\tau_{ep}^{-1} \propto D/L_{ep}^2 \propto T^2$, and therefore the electron-phonon length (17) is inversely proportional to the temperature.

The procedure of extracting the detailed form of τ_{ep}^{-1} or L_{ep} from the experimental results is as follows. First, the value of η is obtained by fitting the $R(F, T)$ data of Fig. 1 to Eq. (20), as shown in the bottom panel of this figure. Note that the latter needs the parameter γ as input. This is defined by Eq. (19) above and is thus obtained from the near-equilibrium $R(T)$ measurement performed on the same sample. Such $R(T)$ data and their associated γ are shown in Fig. 2 for two samples. These are made from the same batch of a Au-doped $\text{In}_2\text{O}_{3-x}$ film, they only differ in their lateral dimensions. The first is the $3500 \mu\text{m}$ sample of Fig. 1. The second sample is $80 \mu\text{m}$ long. The sheet resistances of the two are within 1% of each other, yet their logarithmic slopes are somewhat different. Also, both samples show a systematic deviation from the theoretical $\ln(T)$ dependence, a feature that seem to occur in some other 2D systems.²⁵ Since we are mainly interested in the restricted temperature range 0.28–1 K, this feature

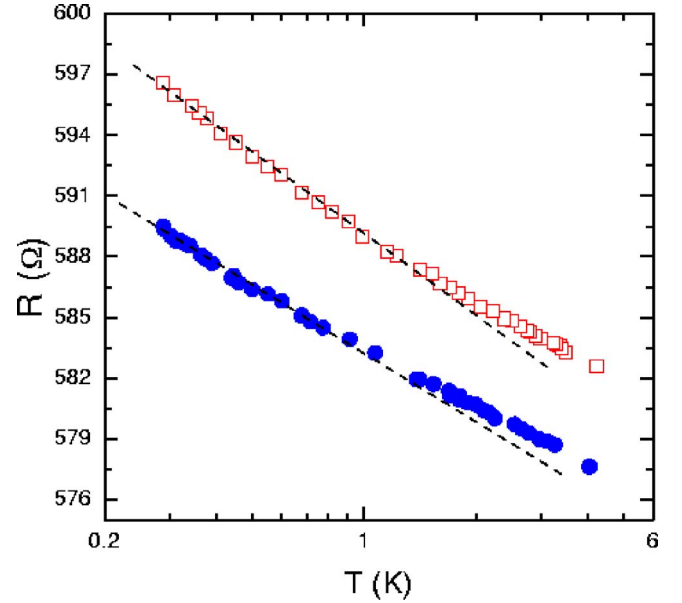


FIG. 2. (Color online) Resistance versus temperature for the sample of Fig. 1 (open squares) and for a $\text{In}_2\text{O}_{3-x}:\text{Au}$ sample with length $L=80 \mu\text{m}$ and width $W=500 \mu\text{m}$ (full circles). The dashed lines are the logarithmic slopes used in defining the value of γ [see Eq. (19)].

may be ignored, and γ is defined by fitting $R(T)$ to a simple $\ln(T)$ over the relevant range as shown in the figure. The fits yield $\gamma \approx 0.0098$ and $\gamma \approx 0.0081$ for the long and short samples respectively, and these values are used in the subsequent analysis below.

The 2D nature of transport in the samples used here is natural for the temperature regime studied: The relevant length scale for the Altshuler-Aronov corrections to the conductivity is $L_T = (\hbar D / k_B T)^{1/2}$. For $T \leq 4$ K, $L_T \geq 300 \text{ \AA}$, using $D = 8.56 \text{ cm}^2/\text{sec}$ as measured for these samples. This scale thus exceeds the sample thickness (200 \AA) at all temperatures relevant to the present study rendering the samples effectively 2D with respect to electron-electron interactions. The WL corrections are characterized by the length scale L_ϕ which is typically 10 times bigger (Ref. 18) therefore the case for a 2D behavior is quite natural from this aspect as well. We also note that the elastic mean-free-path l associated with $D = 8.56 \text{ cm}^2/\text{s}$ is about 50 \AA which is at least an order of magnitude smaller than any reasonable estimate of the thermal phonon wavelength at $T < 4$ K thus these samples are deep in the dirty limit.

An excellent fit to the data in the bottom panel of Fig. 1 can be obtained using Eq. (20) with $\eta = 3.7 \times 10^{55} \text{ 1/J}^2 \text{ m}^2$, $\gamma = 0.0098$ and $p=2$. The use of this formula, appropriate for the $L \gg L_{ep}$ limit, is justified for this sample as can be seen by estimating L_{ep} . Inserting the above value of η in Eq. (17), gives $L_{ep} \approx 20 \mu\text{m}$ at 1 K and only $L_{ep} \approx 60 \mu\text{m}$ at $T \approx 0.28$ K. Thus L_{ep} is much smaller than L down to the low-temperature we are dealing with here.

For the $80 \mu\text{m}$ sample, on the other hand, a crossover to the short-sample regime is realized in the temperature interval covered in our experiments. The crossover can be seen by studying the data depicted in Figs. 3 and 4. Figure 3

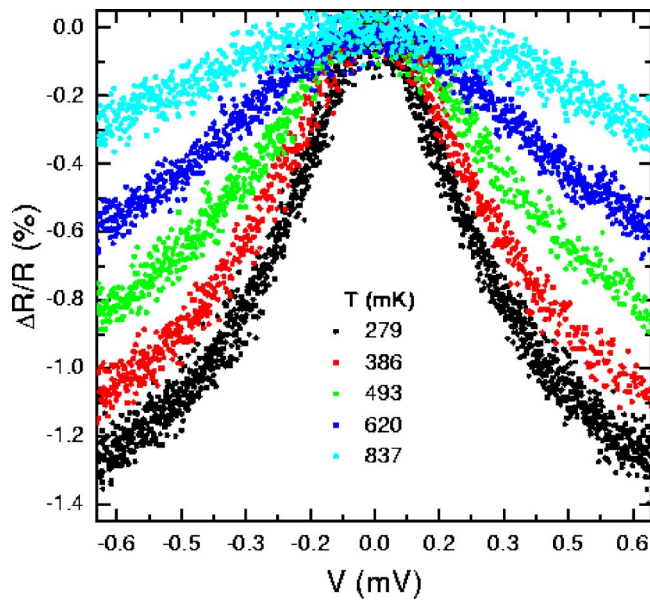


FIG. 3. (Color online) Dependence of the differential resistance on voltage at several temperatures. $\text{In}_2\text{O}_{3-x}:\text{Au}$ sample with length $L=80 \mu\text{m}$ and width $W=500 \mu\text{m}$. The noisier data here (as compared with those of Fig. 1), is mainly due to the much smaller sample size.

shows the raw $R(V)$ data measured at different temperatures. Figure 4 shows these data plotted according to the short-sample formula [Eq. (22)] in the top panel, and according to the long-sample scheme [Eq. (20) with $p=2$] in the bottom panel. The crossover temperature is the temperature below which the $R(F, T)$ data can be scaled as a function of V/T , and above which it scales as F/T^2 . Comparison of the top and bottom panels of Fig. 4 shows it is evident that this temperature is approximately 0.5 K. Thus, with this sample, the consistency of our approach can be tested in the two limits. As shown in the top panel of Fig. 4, a good fit to the $\Delta R/R(0)$ data is obtained using Eq. (22), which involves just the parameter γ . Note that the best fit γ is quite close to the γ that one gets from the logarithmic fit to the $R(T)$ data of this sample (Fig. 2). The other limit, which conforms to Eq. (20), also yields a reasonable agreement, with the *same* γ as used above, and with $\eta=2.2 \times 10^{55} \text{ 1/J}^2 \text{ m}^2$ (see bottom panel of Fig. 4). The quality of the fit here is less good than in the $3500 \mu\text{m}$ sample, perhaps due to the fact that even at the highest temperature used the sample is not really in the long-sample limit.

Finally, using the value of η for this sample in Eq. (17), one gets $L_{ep} \approx 34 \mu\text{m}$ at 1 K and $\approx 100 \mu\text{m}$ at $T \approx 0.28$ K. Since it is plausible to expect that the crossover from the short-sample to long-sample regime should occur when L_{ep} becomes comparable with $L/2$, these numbers are consistent with our picture.

We turn now to discuss the physics that underlies the $\tau_{ep}^{-1} \propto T^2$ law for the electron-phonon scattering rate suggested by our analysis. It is important to note that the enhanced electron-phonon inelastic scattering resulted from the inclusions of Au atoms in the indium-oxide matrix: By comparison, an undoped $\text{In}_2\text{O}_{3-x}$ sample showed τ_{ep}^{-1} that, at T

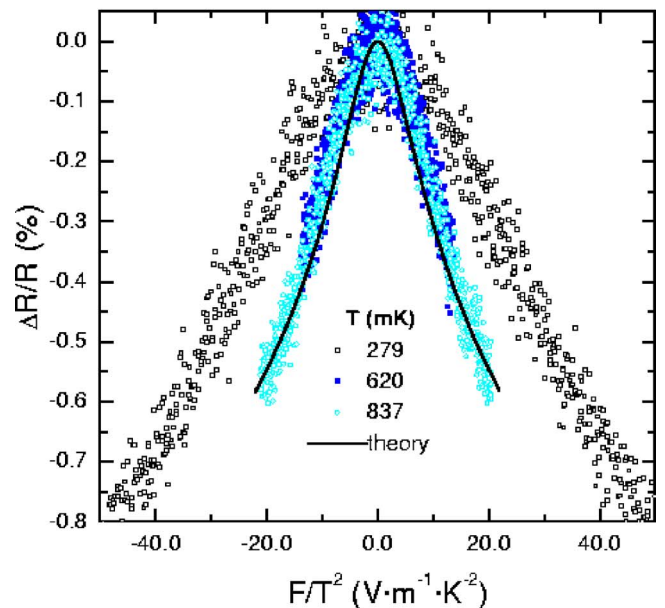
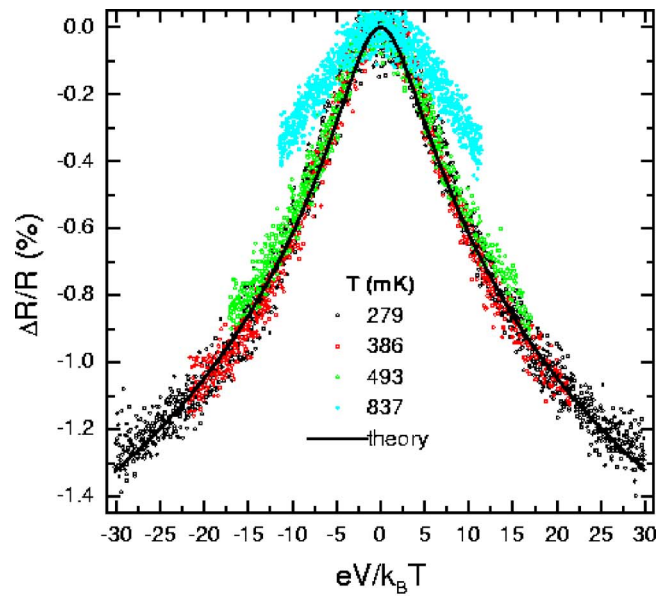


FIG. 4. (Color online) Top panel: The differential resistance versus the voltage V normalized by the temperature T using the data of Fig. 3. The full line is a best fit to the data using Eq. (22). Note the data collapse for the three lowest temperatures and the deviations from the short-sample behavior at $T=837$ mK. Bottom panel: Data from the same figure (Fig. 3) plotted as a function of $F (=V/L)$ normalized by T^2 . The full line is a best fit to the data using Eq. (20). Note the data collapse for the two highest temperatures and the deviations from the long-sample behavior at $T=279$ mK. For clarity of presentation, the data for $T=620$ mK (386 mK) were eliminated from the top (bottom) panels, respectively.

≈ 0.5 K, was more than three orders of magnitude smaller¹⁸ [in fact, L_e in the undoped samples was larger than the sample length for $T \leq 1$ K, making it obey the short-sample scaling Eq. (22), see Ref. 18, Fig. 14]. Since these “pure” and the Au-doped samples had otherwise quite similar parameters (their R_{\square} , and diffusion constant are the same to

within 40%), the nontrivial role of the gold in enhancing τ_{ep}^{-1} must be considered.

It seems likely that the enhanced electron-phonon scattering rate is a manifestation of the Sergeev-Mitin mechanism for electron-phonon scattering in disordered metals. The gold impurities in our samples are heavier than the host atoms, and being inert they are also loosely attached to the indium-oxide lattice. These factors limit their ability to follow the lattice movement, and thus the main assumption of the Sergeev-Mitin mechanism is fulfilled. At the same time, the Au atoms are active as local soft-modes which could be very effective in dephasing the electrons.²⁶ However, being weakly coupled to the lattice, they cannot efficiently dissipate the energy, gained by inelastic collisions with the electrons, to the bath. Therefore the Au inclusions contribute to dephasing much more than to energy relaxation. Note indeed that the phase coherence length in these samples is dominated by the interaction of the electrons with these local modes¹⁸ and it is $\approx 0.4 \mu\text{m}$ at $T=0.3 \text{ K}$ as compared with $L_{ep} \approx 100 \mu\text{m}$. That the dephasing rate exceeds the energy relaxation rate by many orders of magnitude is quite a general property of low temperature transport, which follows from the different temperature dependencies of energy relaxation processes, on the one hand, and dephasing, on the other hand.

To summarize, we have employed a scaling analysis of nonohmic resistance curves in order to extract the electron-phonon scattering rate of metallic films. The method makes use of the temperature dependence of the resistivity therefore it is best suited for those cases where the resistance can be used as a sensitive thermometer. Our theoretical results for quasi-two-dimensional samples may be easily generalized to other dimensionalities. In these cases the temperature dependence of the resistance, at sufficiently low temperatures, is dominated by a power law behavior, $R(T)=R_D(1-\gamma T^\nu)$.

From here it follows that the scaling function (1) of long samples satisfies the relation

$$T^{-\nu} \Delta \mathcal{R} = \gamma \left[1 - \left(1 + \frac{(eF)^2}{\eta T^{p+2}} \right)^{\nu/(p+2)} \right].$$

Having the equilibrium parameters (γ and ν), the experimental data of $R(T, F)$ can be fitted to the above form and both η and p can be extracted. The electron phonon length is then deduced from Eq. (17).

We reiterate that in order to apply the scaling approach, the following conditions should be satisfied: (a) the heat transfer from the electrons to the bath is dominated by the electron-phonon collisions and (b) the electron-electron diffusion length should be much smaller than the energy relaxation length. On the other hand, the scaling approach is insensitive to the inclusion of other ingredients such as two level systems and Kondo impurities as long as they do not serve as additional channels for heat conduction to the bath. Furthermore, for long samples the quality of the contacts is of minor importance, since the amount of heat transferred by the electrons through the contacts is anyhow negligible. For short samples, however, our analysis assumes that the electrons near the contacts are at the bath temperature. This means that the contacts are ideal heat sinks, a caveat that should be borne in mind when using contacts made of a superconducting material.

ACKNOWLEDGMENTS

The authors gratefully acknowledge discussions with I. Aleiner and Y. Imry. This work has been supported in part by the Israel Science Foundation (ISF) and by the German-Israel Foundation (GIF).

¹A. Schmid, Z. Phys. **259**, 421 (1973).

²A. B. Pippard, Philos. Mag. **46**, 1104 (1955).

³M. Yu. Reizer and A. V. Sergeev, Zh. Eksp. Teor. Fiz. **90**, 1056 (1986) [Sov. Phys. JETP **63**, 616 (1986)].

⁴M. E. Gershenson, D. Gong, T. Sato, B. S. Karasik, and A. V. Sergeev, Appl. Phys. Lett. **79**, 2049 (2001).

⁵J. T. Karvonen, L. J. Taskinen, and I. J. Maasilta, Phys. Status Solidi C **1**, 2799 (2004); Phys. Rev. B **72**, 012302 (2005).

⁶P. Kivinen, M. Prunnila, A. Savin, P. Torma, J. Pekola, and J. Ahopelto, Phys. Status Solidi C **1**, 2848 (2004).

⁷M. L. Roukes, M. R. Freeman, R. S. Germain, R. C. Richardson, and M. B. Ketchen, Phys. Rev. Lett. **55**, 422 (1985).

⁸A. K. M. Wennberg, S. N. Ytterboe, C. M. Gould, H. M. Bozler, J. Klem, and H. Morkoc, Phys. Rev. B **34**, 4409 (1986).

⁹P. M. Echternach, M. R. Thoman, C. M. Gould, and H. M. Bozler, Phys. Rev. B **46**, 10 339 (1992).

¹⁰F. C. Wellstood, C. Urbina, and J. Clarke, Phys. Rev. B **49**, 5942 (1994).

¹¹G. Bergmann, W. Wei, Y. Zou, and R. M. Mueller, Phys. Rev. B **41**, 7386 (1990).

¹²J. F. DiTusa, K. Lin, M. Park, M. S. Isaacson, and J. M. Parpia, Phys. Rev. Lett. **68**, 1156 (1992).

¹³P. W. Watson III and D. G. Naugle, Phys. Rev. B **51**, 685 (1995).

¹⁴C. Y. Wu, W. B. Jian, and J. J. Lin, Phys. Rev. B **57**, 11232 (1998).

¹⁵D. Belitz and M. N. Wybourne, Phys. Rev. B **51**, 689 (1995).

¹⁶W. Jan, G. Y. Wu, and H.-S. Wei, Phys. Scr. **71**, 552 (2005).

¹⁷A. Sergeev and V. Mitin, Phys. Rev. B **61**, 6041 (2000).

¹⁸Z. Ovadyahu, Phys. Rev. B **63**, 235403 (2001).

¹⁹P. W. Anderson, E. Abrahams, and T. V. Ramakrishnan, Phys. Rev. Lett. **43**, 718 (1979).

²⁰M. R. Arai, Appl. Phys. Lett. **42**, 15 (1983).

²¹K. E. Nagaev, Phys. Lett. A **169**, 103 (1992); K. E. Nagaev, Phys. Rev. B **52**, 4740 (1995).

²²V. I. Kozub and A. M. Rudin, Phys. Rev. B **52**, 7853 (1995).

²³G. Bergmann, Phys. Rep. **107**, 1 (1984).

²⁴B. L. Altshuler and A. G. Aronov, in *Electron-Electron Interaction in Disordered Systems*, edited by A. L. Efros and M. Pollak (North-Holland, Amsterdam, 1985).

²⁵R. M. Mueller, R. Stasch, and G. Bergmann, Solid State Commun. **91**, 255 (1994).

²⁶Y. Imry, Z. Ovadyahu, and A. Schiller, cond-mat/0312135 (unpublished).